Insights from Magnetic and Geologic Observations in Mars' Southern Hemisphere Crust. C. A. Milbury[1] (cmilbury@ucla.edu), C. L. Johnson[2], and G. Schubert[1,3], [1]UCLA, Department of Earth and Space Sciences, 595 Charles Young Drive East, Los Angeles, CA 90095-1567, [2]Earth and Ocean Sciences, University of British Columbia, Vancouver, BC V6T 1Z4 Canada; IGPP, Scripps Institution of Oceanography, 9500 Gilman Drive, La Jolla, CA 92093 United States, [3]Institute of Geophysics and Planetary Physics, UCLA, Los Angeles, CA 90095-1567.

Introduction: Johnson and Phillips [1] used magnetic field observations from Mars Global Surveyor, the ages of geologic units, and topographic data to provide constraints on the thermal and magmatic evolution of the Tharsis volcanic province on Mars. They conclude that Tharsis is underlain by a Noachian crust that was previously more magnetic than at present.

In this paper we extend this analysis to the ancient crust in Mars' southern hemisphere to test for differences in the distributions of the observed magnetic field from that predicted by a dipolar magnetic field model. We examine the portion of crust that has not been affected by large-scale crustal modification. In particular, we exclude the Tharsis complex, and the Hellas, Argyre, and Isidis impact basins because they have clearly been affected by thermal and magmatic modification that has occurred since the formation of the crust. Figure 1 shows the geologic [2], and magnetic field [3] maps with the boundaries of the excluded regions outlined in black.

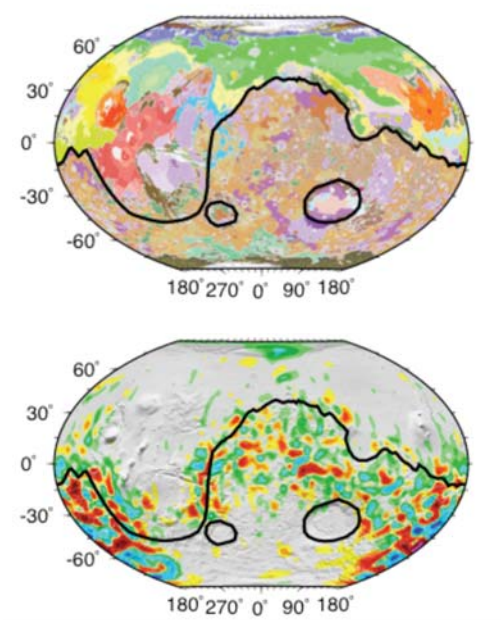

Figure 1. Geologic (top) [2] and magnetic field [3] maps (bottom). The black line delineates the southern hemisphere region analyzed, excluding the Hellas and Argyre basins.

Methodology: We investigate the distributions of magnetic field intensities as a function of geological age, where the latter is assessed via global maps of surface unit ages [2]. Available global geological maps have higher spatial resolution (0.125°) compared with global magnetic field [3, 4] models (2° at best). The geologic data are grouped into bins of the same size as the magnetic field data and a modal age is assigned to the bin. In the analysis shown here we use 1° bins. Although not shown here, bins of 2° and 3° produce similar results. We use the radial component of the magnetic field, since it is least affected by external fields. The number of magnetic observations, the mean value, standard deviation, and maximum values are computed for each bin. The observed distribution of magnetic field values are compared with the distribution predicted by a dipolar magnetic field. The predicted values are analyzed in the same geographical region as the data. This is done for an array of paleopole positions.

Results: Table 1 summarizes the results of the analysis for the observations and selected paleopole positions. Magnetic field values of less than 10 nT have been excluded. Statistics for cut-offs of 0 and 25 nT have been investigated, but are not shown here. Table 1 shows that the lowest maximum magnetic field values occur in the Amazonian crust, and the highest values occur in both the Noachian and Hesperian crusts. The highest number of magnetic field observations occur in Noachian crust, and the lowest in the Amazonian crust, which is expected since most of the youngest portions of the crust have been removed from the analysis. The standard deviation is comparable to the mean value, but it is an order of magnitude lower than the maximum value.

Mag Model	*num B obs*	*mean B (nT)*	*std dev (nT)*	*max B (nT)*
Purucker et al., 2000	10975/3141/1652	56/53/59	68/67/60	664/645/286
Rotation axis Model	18220/6540/3613	357/424/614	188/197/76	637/639/641
Equatorial	18118/6498/3265	295/263/87	177/188/104	648/647/647

Table 1. The number of observations, mean value, standard deviation, and maximum value for the radial magnetic field component for 1° bins. The values are given in the following format: Noachian/Hesperian/Amazonian. The magnetic field model is given in the far left column.

The histogram and cumulative distribution function (CDF) for the magnetic field model of Purucker et al.

[4] are shown in Figure 2 below. Statistics for the model of Langlais et al. [3] are not shown here, but are similar.

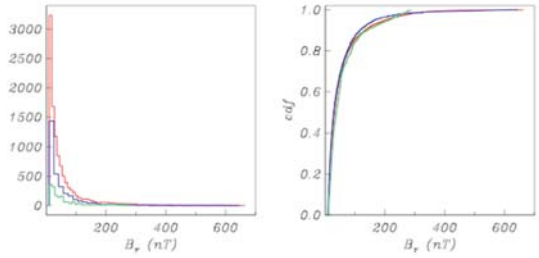

Figure 2. Histogram (left) and CDF (right) for the absolute value of the radial component of the magnetic field from the model of [4] over Amazonian (green), Hesperian (blue) and Noachian (red) surface units. Values of B_r less than 10 nT are excluded.

The histogram and CDFs for the rotation axis and equatorial dipolar magnetic field models are given in Figure 3 below. The statistics for the rotation axis dipolar magnetic field model do not correspond well with the observed statistics of Figure 2. The equatorial dipolar magnetic field model provides a better fit. In particular, the Amazonian statistics correspond well.

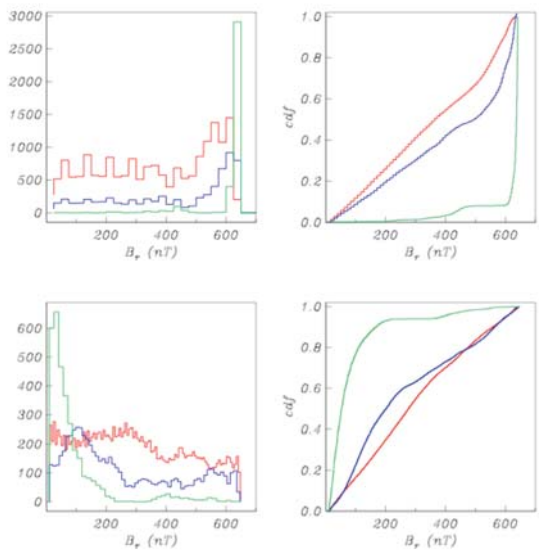

Figure 3. Same as Figure 2, but for rotation axis (top) and equatorial (bottom) dipolar magnetic field models.

The distribution of the age of geologic units with latitude is given in Figure 4 below. It shows that most of the Amazonian units are located near the rotational pole.

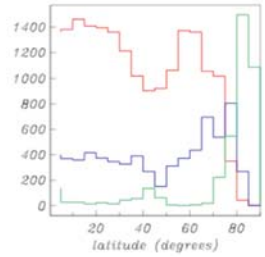

Figure 4. The histogram for the distribution of the geologic age of units with the absolute value of latitude.

Conclusions: The maximum values of the magnetic field given in Table 1 for the Noachian and Hesperian units are essentially the same. The Amazonian units have lower magnitude magnetic field values than that the Noachian and Hesperian units. Possible explanations include signals from underlying Noachian-age basement (either alone, or via a contribution to secondary magnetization of overlying Amazonian crust); magnetization by a late, weak field; or a dynamo that extended beyond the end of the Noachian. The Amazonian statistics for the equatorial dipolar magnetic field model correspond well to the observed statistics. Dipolar magnetic field models for other paleopole positions might yield statistics in better agreement with the observed statistics of the Noachian and Hesperian crusts. Future work will systematically investigate an array of paleopole positions.

References: [1] Johnson, C. L. and Phillips, R. J. (2005) *EPSL,* 230 241– 254. [2] Scott, D.H., Tanaka, K.L., USGS Map I-1 802-A (1986). [3] Langlais, B., et al. (2004) *JGR., 109(E02008),* doi:10.1029/2003JE002048. [4] Purucker, M., et al., *GRL*, *27* (2000) 2449–2452.